Density-of-states of crystalline 2,2'-bithiophene: *ab initio* analysis and comparison with inelastic neutron scattering response

2004 J. Phys.: Condens. Matter 16 7385

(http://iopscience.iop.org/0953-8984/16/41/018)

INSTITUTE OF PHYSICS PUBLISHING JOURNAL OF PHYSICS: CONDENSED MATTER

J. Phys.: Condens. Matter **16** (2004) 7385–7396 PII: S0953-8984(04)83071-6

Density-of-states of crystalline 2,2′-bithiophene: *ab initio* analysis and comparison with inelastic neutron scattering response

P Hermet[1,4], **J-L Bantignies**[1], **A Rahmani**[1,2], **J-L Sauvajol**[1] **and M R Johnson**[3]

[1] Groupe de Dynamique des Phases Condensées (UMR CNRS 5581), Université Montpellier II, 34095 Montpellier Cédex 5, France
[2] Département de Physique, Université MY Ismail, Faculté des Sciences, BP 4010, 50000 Meknès, Morocco
[3] Institut Laue-Langevin, BP 156, 38042 Grenoble Cédex 9, France

E-mail: hermet@gdpc.univ-montp2.fr

Received 29 June 2004, in final form 16 September 2004
Published 1 October 2004
Online at stacks.iop.org/JPhysCM/16/7385
doi:10.1088/0953-8984/16/41/018

Abstract

Phonons in the crystalline phase of 2,2′-bithiophene (2T) are investigated using the *direct method* combined with density functional theory (DFT)-based total energy calculations. Phonon calculations are performed as a function of the long range interactions and the displacement amplitude used for calculating Hellmann–Feynman forces. For the first time, we show that both these parameters are crucial in simulating accurately the experimental low-frequency density-of-states of the 2T crystalline phase, obtained from inelastic neutron scattering experiments. The DFT/*direct method* approach allows the anharmonicity of phonons to be investigated. The anharmonic behaviour of the low-frequency vibrational modes (below 300 cm^{-1}) as the high-frequency vibrational modes at 685, 800 and 885 cm^{-1} of the 2T crystalline phase is clearly demonstrated. Except for these three latter high-frequency modes, a harmonic behaviour is observed for the intramolecular modes. The calculation of the multiphonon contribution predicts the appearance of a broad background in the 600–1500 cm^{-1} frequency range, as well as defined features around 950 and 1130 cm^{-1}, in good agreement with the inelastic neutron scattering data. Finally, low-frequency dispersion curves are given.

(Some figures in this article are in colour only in the electronic version)

[4] Author to whom any correspondence should be addressed.

1. Introduction

In conjugated polymers based on thiophene groups, the presence of long range delocalization of π-conjugated systems on neighbouring rings governs their optical and conducting/semiconducting properties [1, 2]. Of particular interest are the phonons in the solid state of these systems because these dynamics can promote or hinder the π–π^* overlap which is directly correlated to the electronic transport. In polyheterocycles such as polythiophene (polyaniline), the rotational degrees of freedom (librons) of the thienyl(phenyl)-ring couple to the electrons via the electron–libron coupling, which is expected to play an important role in the physics of these conjugated polymers [3–5]. In this context, we seek a clear understanding of the low-frequency spectral region (external modes and librons) of conjugated polymers in the crystalline phase.

2,2′-bithiophene (2T) is considered as the reference compound of conjugated polymers, with the advantage of being experimentally stable under ambient conditions [6, 7]. The experimental phonon density-of-states (DOS) of 2T in the crystalline phase has been measured by inelastic neutron scattering (INS) at low temperature [8]. *Ab initio* simulations of the INS spectrum of a 2T isolated molecule were performed by Degli Esposti *et al* [8, 9]. Good agreement was found between experimental and calculated frequencies for the intramolecular modes in the 300–1600 cm^{-1} frequency range. Nevertheless, because the intermolecular interactions were not taken into account in the calculations, the intensity of the experimental INS spectrum was not accurately reproduced. Recently, *ab initio* simulations of the INS spectrum of the 2T crystalline phase, including intermolecular interactions, were performed and they have led to a better agreement with experimental intensity of the INS spectrum in the intramolecular phonon range [10]. However, a number of computational parameters which affect the convergence of the intermolecular force constants, and therefore the low-frequency phonons (below 300 cm^{-1}), were not investigated. Consequently, there is no accurate experimental or theoretical assignment of the low-frequency modes of the 2T crystalline phase in the literature.

Although density functional theory (DFT) [11] is considered nowadays as the standard method for simulating the properties of solids from first principles [12–15], there are few articles in the literature which simulate the INS low-frequency phonon spectra of large molecules in the solid state. The main reasons arise from the high computational cost that is required to obtain adequate numerical precision in such calculations.

In this work, we are primarily interested in simulating the low-frequency phonon dynamics in the crystalline phase of 2T by first-principles calculations using DFT coupled to the *direct method*. This approach allows intermolecular, long range interactions to be investigated using the supercell method, and the dependence of vibrational modes on the magnitude of atomic displacements used in the calculations of the Hellmann–Feynman forces to be probed.

This paper is organized as follows. In section 2, we describe in detail the computational method for calculating vibrational INS spectra. Section 3 presents the results of our first-principles calculations. We compare our calculated structural geometry relaxation on the 2T crystalline phase and on the isolated molecule with x-ray diffraction experiment. Calculated INS spectra, including multiphonon contributions, are compared to INS experiments. For the discussion, the analysis of the low-frequency INS spectra has been separated from that of the high-frequency ones. An evaluation of the anharmonicity of phonon modes is investigated. Representation of the Γ-point ($\mathbf{q} = \mathbf{0}$) normal modes with their symmetry and dispersion curves related to the low-frequencies of the 2T crystalline phase are given. In this section, all simulation parameters are considered and their influence on the calculated INS spectrum are investigated in detail. In this sense, the present paper is considered as a reference article

in our future low-frequency INS simulations of conjugated oligomers in the crystalline phase. Finally, section 4 concludes the paper.

2. Computational method

There are basically two methods for calculating vibrational INS spectra of crystalline solids from first-principles: the *linear response method* [16] and the *direct method* [17]. The main goal of these methods is the calculation of the dynamical matrix which represents the fundamental quantity for understanding vibrational dynamics of materials. In the *linear response method*, the dynamical matrix is obtained from the modification of the electronic density, via the inverse dielectric matrix, resulting from the phonon displacement of atoms. The dielectric matrix is calculated from the eigenfunctions and energy levels of the unperturbed system. The dynamical matrix can be determined at any wavevector in the Brillouin zone, with a computational effort comparable to a ground state optimization. Only linear effects, such as harmonic phonons, are accessible with this technique. However, the computational cost restricts the *linear response method* to systems containing only a few tens of atoms per unit cell [18]. In the case of the *direct method*, there exist two variants. In the first variant, the so-called *frozen-phonon method*, the dynamical matrix is calculated as a function of the displacement amplitude in terms of the difference between the energies of the distorted and ideal lattices. The second variant of the *direct method* uses the forces related to the displacements of the atoms in a supercell calculated via the Hellmann–Feynman (HF) theorem to derive the force constant matrix, and hence the dynamical matrix. The implementation of the *direct method* is rather straightforward and allows the study of anharmonic force constants to any order. However, strictly speaking, this method is restricted to wavevectors for which the phonon displacement pattern is commensurate to the supercells used in the calculations. In reality, the phonon calculation is converged if the supercell is large enough for the forces on atoms at the cell boundary to be effectively zero when the atom in the centre of the supercell is displaced from equilibrium.

2.1. Crystalline phase

Calculations of the vibrations in the crystalline phase of 2T were performed using the Vienna *ab initio* simulation package (VASP) [19–21]. Exchange–correlation effects were handled within the generalized gradient approximation (GGA) as proposed by Perdew, Burke and Ernzerhof (PBE) [22]. The interaction between ions and electrons was described by the projector augmented wave (PAW) method [23] in the real space representation. Generally, the PAW potentials are more accurate than the ultrasoft pseudopotentials (US-PP) because they reconstruct the exact valence wavefunction with all nodes in the core region. The energy cutoff for plane-wave calculations was 280 eV. The unit cell of 2T [24] ($n = 32$ atoms) was used as input in the optimization procedure of the structure ('1-cell' model). Only the atomic coordinates were optimized to prevent unphysical expansion of the unit cell due to the lack of long range dispersive interactions in DFT-based methods. In addition to this single unit cell model, we have considered three supercells made by doubling the single unit cell (i) only along the b crystallographic axis ('2-cell' model), (ii) along the b and a crystallographic axis ('4-cell' model) and (iii) along the three crystallographic axes ('8-cell' model). These supercells contain $2n$, $4n$, $8n$ atoms in boxes of size about $7.7 \times 11.5 \times 8.9$, $15.5 \times 11.5 \times 8.9$, $15.5 \times 11.5 \times 17.9$ Å^3, for the 2-cell, 4-cell and 8-cell models respectively. In practice, we have optimized the structure by using a fine integration grid on the atomic coordinates of the single unit cell until the maximum residual force was less than 3×10^{-4} eV Å^{-1}. The supercells were built from the optimized single unit cell, followed by an additional optimization of the atom

coordinates of each supercell. The Brillouin zone was sampled according to the Monkhorst–Pack scheme [25] by using a $4 \times 4 \times 4$ k-points grid for the single unit cell, while $4 \times 2 \times 4$, $2 \times 2 \times 4$ and $2 \times 2 \times 2$ k-points grids were used for the 2-cell, 4-cell and 8-cell models, respectively. Both energy cutoff and k-points sampling were sufficient for convergence of the calculated responses.

The normal modes of vibration were calculated in the harmonic approximation using the *direct method*. From the optimized structure, each atom of the asymmetric unit was displaced with an optimal magnitude of 0.05 Å along the three Cartesian directions (see section 3). Positive and negative displacements were used to minimize numerical errors related to anharmonic effects. In these conditions, since there is a total of 8 atoms in the asymmetric unit of 2T, 48 distorted structures are generated. The HF forces on the atoms of the asymmetric unit in the supercells were obtained from a single point energy calculation on each perturbed structure. Finally, these forces were given as input to the PHONON program [26] which generates and diagonalizes the dynamical matrix for any point in reciprocal space using the symmetry of the crystal structure. The dynamical matrix, and thus the DOS, was calculated for 10 000 wavevectors chosen at random. The dynamical structure factor was calculated from the DOS for a polycrystalline powder. Finally, the calculated spectrum was convoluted with a Gaussian, with a full width at half maximum (FWHM) fixed at 2% of the energy transfer (close to the instrument resolution in the INS experiment function [8]). The contribution of multiphonons, up to five-phonon processes, in the INS spectrum was evaluated.

2.2. Isolated molecule

DFT calculations were also performed on a 2T isolated molecule by using the GAUSSIAN package [27] with the PBE exchange–correlation functional and the 6-31G(d) basis set. Several authors have shown that the absolute minimum of the torsion energy profile of a 2T molecule has a *trans*-distorted conformation (also known as anti-gauche), with a torsion angle around of 150° [28–30]. So, this geometry was used as input in the optimization procedure of the molecule, and the relaxation was performed until the maximum of residual force was less than 3×10^{-4} eV Å^{-1}. The CLIMAX [31] program was used to calculate the INS spectrum of the 2T molecule from the normal modes. Overtones and combinations were included in the calculations.

In this work, since the identification of calculated modes by comparison with experiment is unambiguous, we have not used a scale factor to correct mode frequencies in our simulations.

3. Results and discussion

3.1. Optimized geometry

2T ($C_8H_6S_2$) crystallizes in the monoclinic space group $P2_{1/c}$ (C^5_{2h}) with two molecules per unit cell [24]. The experimental values of the lattice constants are $a = 7.734$ Å, $b = 5.729$ Å, $c = 8.933$ Å and the monoclinic angle β is equal to 106.72°. The asymmetric unit of 2T is composed of 8 atoms. Experimentally, the centrosymmetric molecule of 2T is planar and the sulfur atoms adopt a *trans* configuration (see figure 1).

Table 1 summarizes the geometric parameters obtained after the atomic relaxation of the 2T isolated molecule and 2T crystalline phase. The atom labels and numbering of 2T relative to table 1 are given in figure 2. Both for the crystalline phase and for the isolated molecule, DFT calculations preserve the aromatic character of 2T. This is reflected by the C_3–C_4 calculated single bond which is longer than the C_2–C_3 and C_4–C_5 calculated double bonds respectively

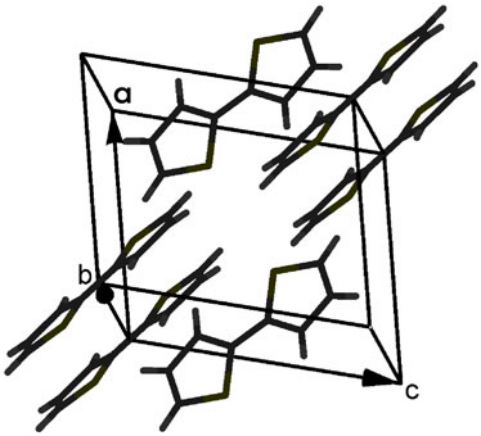

Figure 1. Single crystal of 2T and crystal axis reference system.

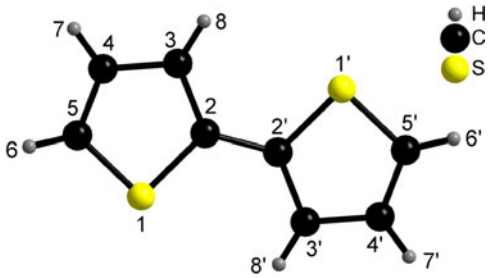

Figure 2. 2T molecule with atom numbering scheme. The molecule belongs to the C_{2h} point group if the rings are coplanar and to the C_2 point group if the rings are twisted. When the rings are coplanar (crystal), the primed atoms are related to the unprimed ones by an inversion centre at the midpoint of the C_2–$C_{2'}$ bond.

Table 1. Optimized structural parameters of 2T for an isolated molecule and for the crystal. The bond lengths are in ångströms, angles and the dihedral angles are in degrees.

	Experimental[a]	Isolated molecule	Crystal[b]
Bonds			
S_1–C_2	1.713	1.759	1.735
C_2–C_3	1.432	1.389	1.392
C_3–C_4	1.444	1.424	1.422
C_4–C_5	1.357	1.378	1.382
C_5–S_1	1.698	1.736	1.715
C_2–$C_{2'}$	1.448	1.449	1.445
Angles			
S_1–C_2–C_3	112.5	110.0	110.3
C_2–C_3–C_4	108.0	113.6	113.0
C_3–C_4–C_5	114.9	112.9	112.5
C_4–C_5–S_1	112.1	111.6	111.6
C_5–S_1–C_2	92.5	92.0	92.6
S_1–C_2–$C_{2'}$	121.2	120.6	120.8
C_3–C_2–$C_{2'}$	126.4	129.4	128.9
Dihedral angles			
S_1–C_2–$C_{2'}$–$S_{1'}$	180.0	161.1	180.0
C_3–C_2–$C_{2'}$–$C_{3'}$	180.0	161.8	180.0

[a] From x-ray diffraction on crystal [24].
[b] For the 8-cell model.

by 0.030 and 0.040 Å for the crystalline phase, as well as 0.035 and 0.046 Å for the 2T isolated molecule. According to x-ray diffraction data, the C_2–C_3 calculated double bond is longer than the C_4–C_5 one, which indicates that the two double bonds are inequivalent and the thiophene ring is asymmetric. Reflecting the underestimated C_2–C_3 and C_3–C_4 calculated bond length both in the crystalline phase and isolated molecule, the C_2–C_3–C_4 calculated angle is larger

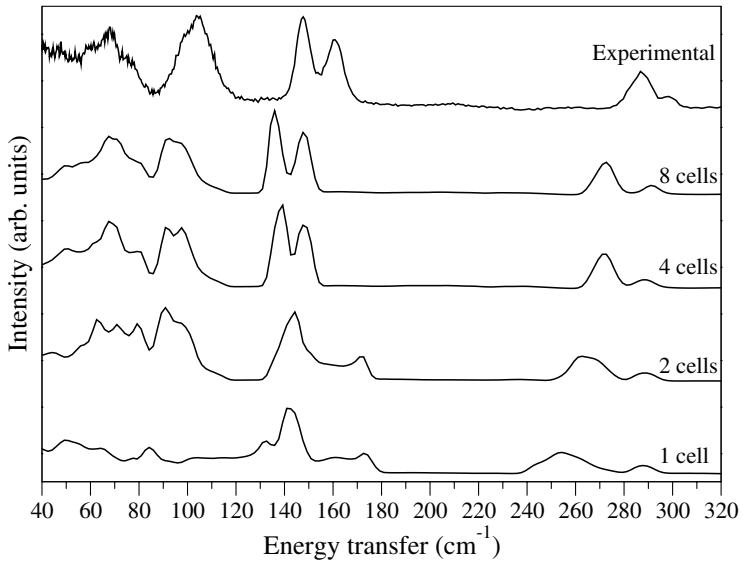

Figure 3. Low-frequency region of the INS spectrum of 2T with calculations using different supercells. Experimental from [8].

than the observed value by 4.6% for the crystalline phase and 5.2% for the isolated molecule. Except for these latter parameters, the differences between the optimized and experimental interatomic distances and angles are about 1–3% for both the crystalline phase and the isolated molecule. Because the dihedral angle S_1–C_2–$C_{2'}$–$S_{1'}$ is respectively equal to 180° in the crystal and to 161.1° in the isolated molecule, the intermolecular interactions due to the crystal packing lead to a planar structure of the molecule. The distance C_2–$C_{2'}$, which represents the inter-cycle distance, is very close to its experimental value.

3.2. Low-frequency region

Since long range intermolecular interactions play an important role in the low-frequency region, one expects to observe major differences in the vibrational modes as a function of the supercell size. In figure 3, we report the calculated INS spectra, in the low-frequency region (40–320 cm^{-1}), for different supercell sizes. The calculated INS spectra are compared with the experimental INS spectrum [8]. We observe a poor agreement between the calculated and experimental spectra for the 1-cell model, since not all long range intermolecular interactions between atoms are included in the calculation. Increasing the supercell size leads to a much better agreement between the calculated and experimental INS spectra. The 2-cell model gives a significant improvement for the bands centred at 68 and 104 cm^{-1}, whereas for the 4-cell and 8-cell models, the agreement is still better, with the doublet at 150 cm^{-1} being correctly reproduced. The intensity distribution from the 8-cell model is the closest to that observed experimentally. As expected, this result demonstrates that the low-frequency modes are very sensitive to the supercell size, and a good evaluation of the long range intermolecular interactions are obtained for a $2 \times 2 \times 2$ supercell.

Low-frequency phonon dynamics are especially sensitive to the molecular crystal packing. The good agreement between the INS spectrum calculated for the 8-cell model and the experimental INS spectrum therefore confirms the crystalline structure of 2T proposed by Pelletier *et al* [24] (figure 3). Moreover, these results demonstrate that long range dispersive interactions, that are absent in the DFT approach, can be compensated for by applying external pressure, that is by fixing the unit cell parameters.

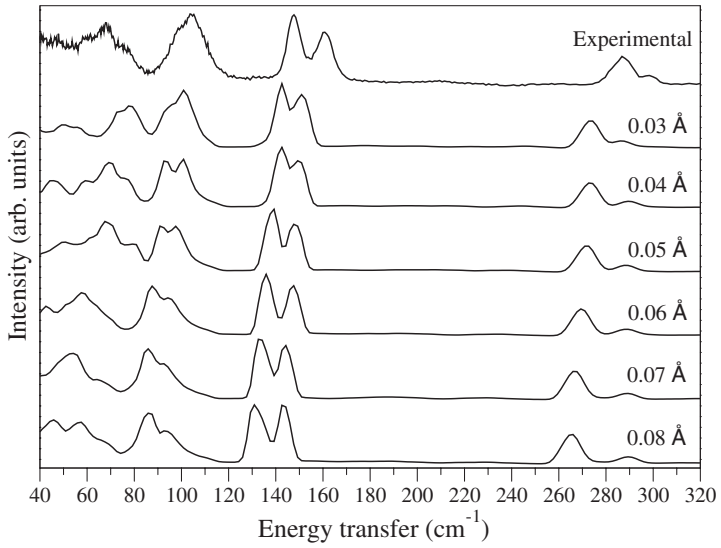

Figure 4. Low-frequency region of the INS spectrum of 2T for the 4-cell model with calculations for different atomic displacements. Experimental from [8].

We have also analysed the effect of the displacement amplitude, used for calculating the HF forces, on the low-frequency INS response. Because the calculation time in DFT methods scales with the third power of the number of atoms, we have performed these calculations in the 4-cell model, which already shows a good agreement with the experimental spectrum, rather than the 8-cell model. The calculations have been performed with different amplitudes in the 0.03–0.08 Å range (figure 4). We observe that the intensity of the low-frequency modes depends significantly on the amplitude of displacement. Much attention should be paid to preserve the linearity of the HF forces as a function of displacement amplitude. Indeed, for displacements which are too small, the forces and numerical noise are of the same order of magnitude, while for large displacements, the linear response theory breaks down. The spectral profile is best reproduced by a displacement equal to 0.05 Å, which reduces the effect of numerical noise in the calculations. For still larger displacements, the equilibrium structure is significantly perturbed and the quality of the calculated spectral profiles decreases.

The downshift of the different calculated modes with the increase of the displacement amplitude reveals the strong anharmonicity of the low-frequency modes (figure 4). Recently, the experimental anharmonicity of the A_u and B_u low-frequency modes has been inferred from the temperature dependence of the infrared spectrum of the 2T crystalline phase [32].

Among all points of the Brillouin zone, the Γ-point is of particular interest because only these modes can be infrared or Raman active. As the structure of 2T is centrosymmetric (point group symmetry C_{2h}), the normal modes at the Γ-point are separated in infrared or Raman active modes. In Raman spectroscopy only modes that transform under symmetry operations as a quadratic form (modes A_g and B_g) are active, whereas in infrared spectroscopy only modes that transform as a vector (modes A_u and B_u) are active. In the low-frequency range, the frequencies and symmetries of the Γ-point normal modes are given in table 2, and their representations are given in figure 5.

Monocrystals of 2T are not available so full dispersion curves cannot be measured. On the basis of the agreement between calculated and experimental INS spectra, the calculated dispersion curves, displayed in figure 9, provide a reasonable picture of the real dispersion curves. This information could be used to calculate all the properties of the 2T crystalline phase in which phonon–phonon and electron–phonon interactions play an important role.

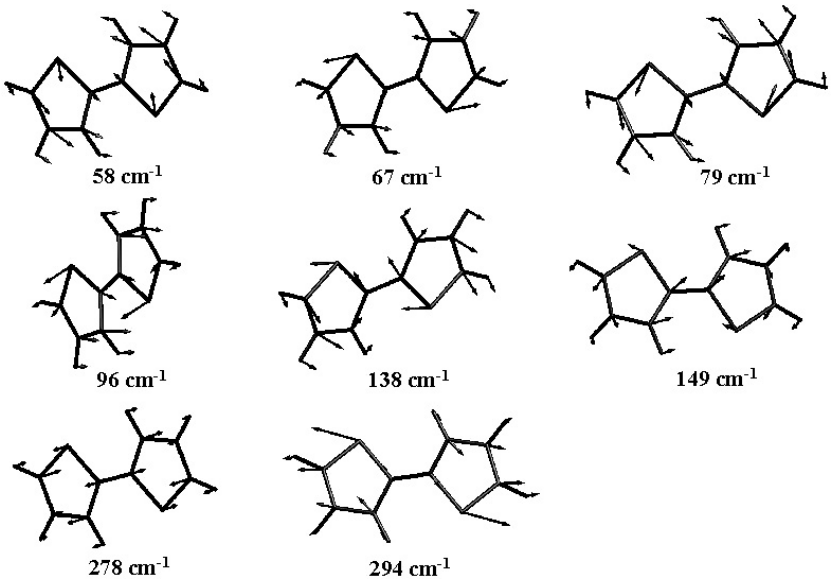

Figure 5. Representation of low-frequency Γ-point normal modes of 2T.

Table 2. Low-frequency Γ-point normal modes of 2T crystal with their multiplicity and symmetry. The frequencies are in cm^{-1}.

Multiplicity	Frequency	Symmetry
1	37	A_u
1	58	A_g
1	66	A_u
1	67	A_g
1	71	B_g
1	79	B_g
1	84	B_u
1	96	B_u
1	99	A_g
1	101	B_g
1	116	A_u
1	132	B_u
1	133	A_u
1	138	B_u
1	149	A_u
1	265	B_g
1	278	A_g
1	290	B_g
1	294	A_g

3.3. High-frequency region

The INS spectrum related to the intramolecular vibrational modes (above 300 cm^{-1}) of the 2T crystalline phase has already been simulated by DFT-based methods [10]. Our calculations are in good agreement with these latter results. In the present study, we focus especially on three specific points: the supercell size effect and the anharmonicity evaluation of the intramolecular

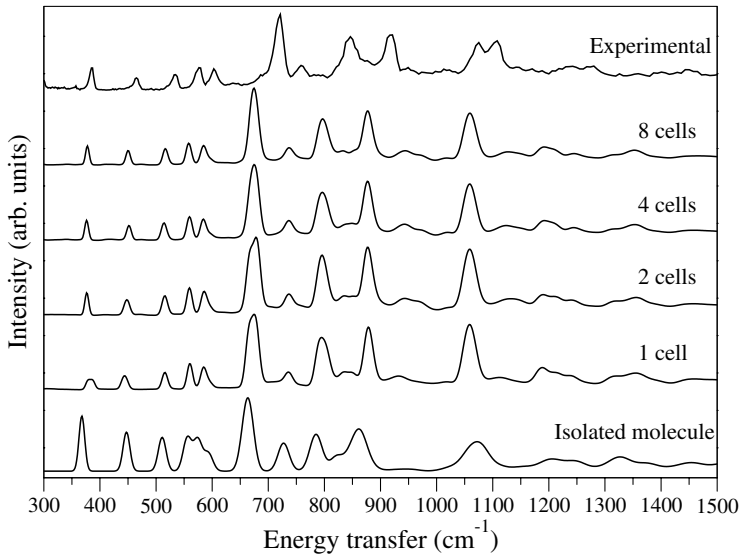

Figure 6. Comparison of the INS spectrum of 2T with calculations for the isolated molecule and for different supercells. Experimental from [8].

modes, as well as the multiphonon contributions to the experimental INS profile. Consequently, our study completes the understanding of the experimental INS spectrum of the 2T crystalline phase related to the high frequencies.

We compare in figure 6 the calculated INS spectra of 2T (isolated molecule and crystalline phase) with the experimental INS spectrum [8]. In the 300–600 cm^{-1} frequency range, the intensities of all vibrational modes are overestimated for the isolated molecule whereas a general good agreement with the experimental intensities is obtained for the 2T crystalline phase. Moreover, the position and intensity of intramolecular modes are insensitive to the supercell size. As expected, these results confirm that the intermolecular interactions between 2T molecules in the crystalline phase contribute weakly to the high-frequency intramolecular modes.

Our calculations fail to reproduce the doublet at 1075 and 1105 cm^{-1} (figure 6). This result could be attributed to a limitation of the GGA functional used in our calculations. Indeed, the same disagreement is found with the Perdew and Wang functional [10] (PW91, functional type GGA), whereas Degli Esposti *et al* [9], by using the hybrid functional B3LYP, found a good agreement with the experimental spectrum in this region. Hybrid functionals are not available in VASP and it would clearly be interesting in the future to perform periodic DFT simulations with the B3LYP or PBE0 functional.

For small displacements, the numerical noise being negligible for the strong force constants at high-frequency, the intensity of the intramolecular modes does not depend significantly on the amplitude of displacements. Larger displacements used in the calculations give worse agreement with the experimental spectrum (figure 7).

The calculated modes at 685, 800 and 885 cm^{-1} present a downshift when the amplitude of the displacement increases, which is an indication of their anharmonicity. Except for these three latter modes, the other intramolecular vibrational modes reveal a harmonic behaviour since their frequency positions are insensitive to the amplitude of displacement used (see figure 7).

The broad contribution which appears in the 600–1500 cm^{-1} frequency range of the experimental INS spectrum is not clearly assigned in the literature (figure 8). Because experiments have been performed at low temperature, only overtones and additive combination

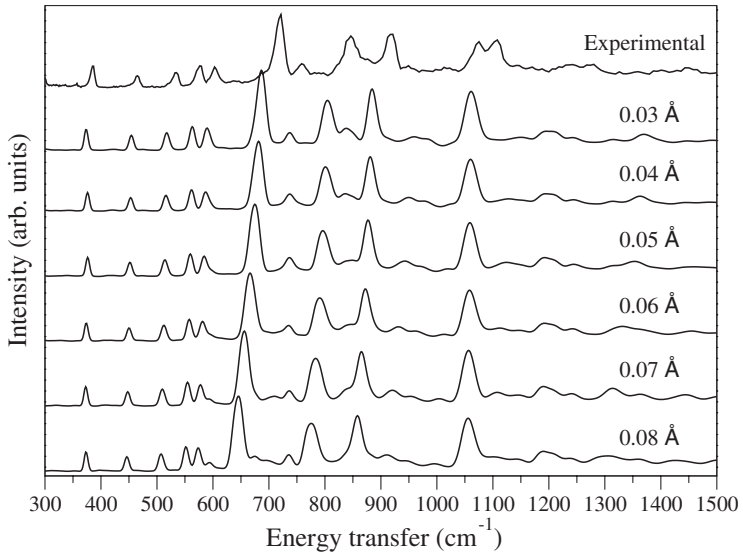

Figure 7. High-frequency region of the INS spectrum of 2T for the 4-cell model with calculations for different atomic displacements. Experimental from [8].

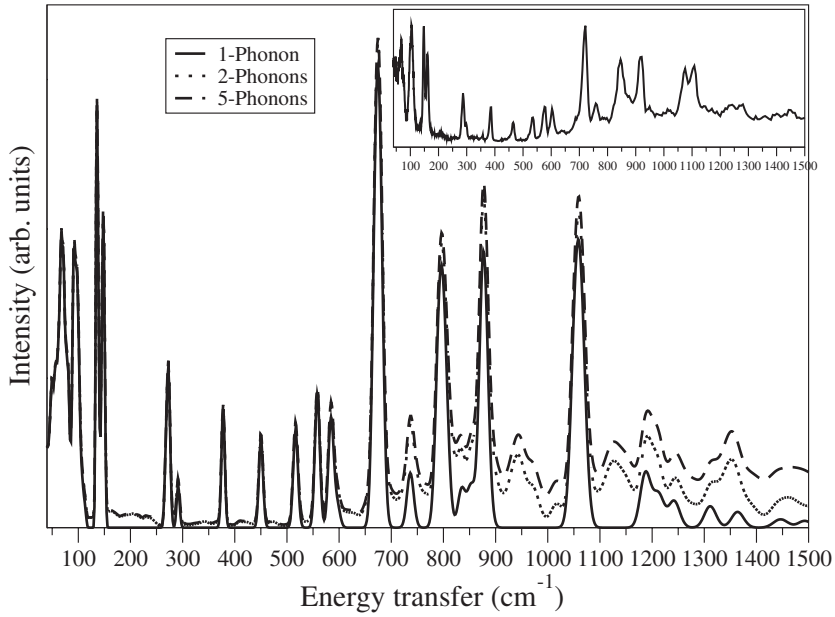

Figure 8. INS spectrum of 2T for one-, two- and five-phonon contributions. Inset: experimental INS spectrum of 2T from [8].

bands contribute to the INS spectrum. We have calculated the multiphonon contributions by taking into account high-order (two to five) phonon scattering processes. Thus, the broad background in the 600–1500 cm^{-1} frequency range is clearly due to multiphonon contributions as are the well-defined features of the experimental spectrum which appear around 950 and 1130 cm^{-1}.

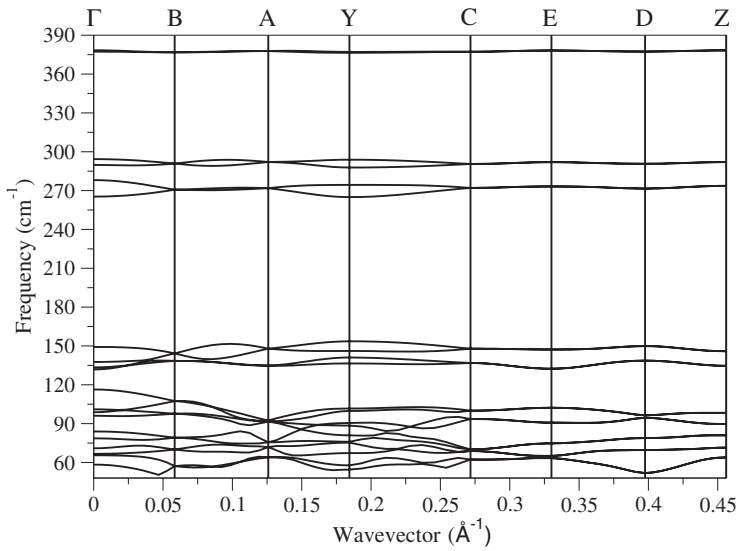

Figure 9. Low-frequency dispersion curves of 2T. The labels (top) denote the high-symmetry points in the Brillouin zone for the monoclinic system.

4. Conclusions

In conclusion, the INS spectrum of 2T in the crystalline phase, including multiphonon processes, has been calculated in a wide frequency range (40–1500 cm^{-1}) by first-principles calculations using DFT in combination with the *direct method*. The geometric parameters of the relaxed atomic structure of 2T crystalline phase are found to be in very good agreement with the experimental ones (at most 3% discrepancy). We have also calculated the low-frequency phonons at the Γ-point of the Brillouin zone with their normal mode representation and symmetry. The excellent agreement with experimental data allows us to assign unambiguously the origin of all the features (first-order and high-order processes) of this spectrum and to predict the dispersion curves of 2T. We assign the broad background in the 600–1500 cm^{-1} frequency range to multiphonon contributions, as the well-defined features of the experimental spectrum which appear around 950 and 1130 cm^{-1}. The roles of the amplitude of the atomic displacements, used in the calculations of the HF forces, and the size of the supercell on the calculation of the low-frequency vibrational dynamics have been demonstrated. The anharmonic behaviour of the low-frequency vibrational modes (below 300 cm^{-1}) as the high-frequency vibrational modes at 685, 800 and 885 cm^{-1} of 2T crystalline phase has been clearly demonstrated. Except for these three latter high-frequency modes, a harmonic behaviour has been observed for the intramolecular modes. These results, obtained at considerable computational cost, also demonstrate that long range dispersive interactions, that are absent in the DFT approach, can be compensated for by applying external pressure, that is, by fixing the unit cell parameters.

Interest in the low-frequency spectrum also stems from the development of far-infrared spectroscopy, making measurements of low-frequency molecular and lattice modes commonplace. Calculations of infrared modes depend on the validity of the eigenmodes which must be established by reproducing the INS spectrum. Using the calculated eigenmodes of 2T, simulations of the far-infrared spectrum, via methods based on Berry's phase (also known

as the modern theory of polarization in the literature [33]) for calculating the Born effective charge tensors, are under investigations.

The computational strategy established in this paper will be extended to longer molecules with a view to obtaining a fuller understanding of the structure and dynamics of polythiophenes. In this context, simulations of INS and infrared spectra in crystalline phases of quater- and sexi-thiophene are in progress.

Acknowledgments

We are grateful to Don Kearley for help with CLIMAX and the CINES (Montpellier, France) for computational facilities (IBM SP3 computers were used).

References

[1] Brédas J-L, Thémans B, André J, Chance R and Silbey S 1984 *Synth. Met.* **9** 265
[2] Katz H E 1990 *J. Mater. Chem.* **7** 369
[3] Ginder J M and Epstein A J 1990 *Phys. Rev.* B **41** 10674
[4] Poussigue G and Benoit C 1989 *J. Phys.: Condens. Matter* **1** 9547
[5] Poussigue G, Benoit C, Sauvajol J-L, Lere-Porte J-P and Chorro C 1991 *J. Phys.: Condens. Matter* **3** 8803
[6] Geiger F, Stoldt M, Schweizer H, Bauerle P and Umbach E 1993 *Adv. Mater.* **5** 922
[7] Garnier F, Horowitz G, Peng X and Fichou D 1990 *Adv. Mater.* **2** 592
[8] Degli Esposti A, Moze O, Taliani C, Tomkinson J T, Zamboni R and Zerbetto F 1996 *J. Chem. Phys.* **104** 9704
[9] Degli Esposti A and Zerbetto F 1997 *J. Phys. Chem.* A **101** 7283
[10] Van Eijck L, Johnson M R and Kearley G J 2003 *J. Phys. Chem.* A **107** 8980
[11] Payne M C, Teter M P, Allan D C, Arias T A and Joannopoulos J D 1992 *Rev. Mod. Phys.* **64** 1045
[12] Fang C M and Metselaar R 2004 *J. Phys.: Condens. Matter* **16** 2931
[13] Lopez G M and Fiorentini V 2003 *J. Phys.: Condens. Matter* **15** 7851
[14] Astala R and Bristowe P D 2002 *J. Phys.: Condens. Matter* **14** 6455
[15] Mukose K, Fukano R, Miyagi H and Yamaguchi K 2002 *J. Phys.: Condens. Matter* **14** 10441
[16] Giannozzi P, de Gironcoli S, Pavone P and Baroni S 1991 *Phys. Rev.* B **43** 7231
[17] Parlinski K 1999 *Am. Inst. Phys. Conf. Proc.* **479** 121
[18] Gonze X, Charlier J-C, Allan D C and Teter M P 1994 *Phys. Rev.* B **50** 13035
[19] Kresse G and Furthmüller J 1996 *Phys. Rev.* B **54** 11169
[20] Kresse G and Furthmüller J 1996 *Comput. Math. Sci.* **6** 15
[21] Kresse G and Hafner J 1993 *Phys. Rev.* B **47** 558
[22] Perdew J P, Burke K and Ernzerhof M 1996 *Phys. Rev. Lett.* **77** 3865
[23] Kresse G and Joubert D 1999 *Phys. Rev.* B **59** 1758
[24] Pelletier M and Brisse F 1994 *Acta Crystallogr.* C **50** 1942
[25] Monkhorst H J and Pack J D 1976 *Phys. Rev.* B **13** 5188
[26] Parlinski K 2001 *Software PHONON* Cracow, Poland
[27] Frisch M J, Trucks G W, Schlegel H B, Scuseria G E, Robb M A, Cheeseman J R, Montgomery J A, Vreven T, Kudin K N, Burant J C, Millam J M, Iyengar S S, Tomasi J, Barone V, Mennucci B, Cossi M, Scalmani G, Rega N, Petersson G A, Nakatsuji H, Hada M, Ehara M, Toyota K, Fukuda R, Hasegawa J, Ishida M, Nakajima T, Honda Y, Kitao O, Nakai H, Klene M, Li X, Knox J E, Hratchian H P, Cross J B, Adamo C, Jaramillo J, Gomperts R, Stratmann R E, Yazyev O, Austin A J, Cammi R, Pomelli C, Ochterski J W, Ayala P Y, Morokuma K, Voth G A, Salvador P, Dannenberg J J, Zakrzewski V G, Dapprich S, Daniels A D, Strain M C, Farkas O, Malick D K, Rabuck A D, Raghavachari K, Foresman J B, Ortiz J V, Cui Q, Baboul A G, Clifford S, Cioslowski J, Stefanov B B, Liu G, Liashenko A, Piskorz P, Komaromi I, Martin R L, Fox D J, Keith T, Al-Laham M A, Peng C Y, Nanayakkara A, Challacombe M, Gill P M W, Johnson B, Chen W, Wong M W, Gonzalez C and Pople J A 2003 *Gaussian 03* Revision B.03 (Pittsburgh, PA: Gaussian)
[28] Yurtsever M and Yurtsever E 2000 *J. Phys. Chem.* A **104** 362
[29] Raos G, Famulari A and Marcon V 2003 *Chem. Phys. Lett.* **379** 364
[30] Karpfen A, Ho Choi C and Kertesz M 1997 *J. Phys. Chem.* A **101** 7426
[31] Kearley G J 1995 *Nucl. Instrum. Methods Phys. Res.* A **354** 53
[32] Hermet P, Bantignies J-L, Rahmani A, Sauvajol J-L, Johnson M R and Serein F 2004 *J. Phys. Chem.* A submitted
[33] King-Smith R D and Vanderbilt D 1993 *Phys. Rev.* B **47** 1651